Atmospheric Environment 63 (2012) 117–124

Contents lists available at SciVerse ScienceDirect

Atmospheric Environment

journal homepage: www.elsevier.com/locate/atmosenv

Determining the influence of different atmospheric circulation patterns on PM_{10} chemical composition in a source apportionment study

Mauro Masiol [a], Stefania Squizzato [a], Daniele Ceccato [b,c], Giancarlo Rampazzo [a], Bruno Pavoni [a,*]

[a] Dipartimento di Scienze Ambientali, Informatica e Statistica, Università Ca' Foscari Venezia, Dorsoduro 2137, 30123 Venezia, Italy
[b] Dipartimento di Fisica "G. Galilei", Università di Padova, Via Marzolo 8, 35100 Padova, Italy
[c] Laboratori Nazionali di Legnaro, Istituto Nazionale di Fisica Nucleare, Viale dell'Università 2, 35020 Legnaro, Padova, Italy

HIGHLIGHTS

- Elements and ions in 193 PM_{10} samples were studied by Positive Matrix Factorization.
- Results were geochemically interpreted in relation to weather data.
- Days with similar circulation patterns were clustered on the basis of wind data.
- Samples with similar air mass histories were grouped using back-trajectories.
- The major components of PM_{10} chemistry and dynamics in NE Italy were identified.

ARTICLE INFO

Article history:
Received 19 March 2012
Received in revised form
11 September 2012
Accepted 12 September 2012

Keywords:
PM_{10}
Atmospheric circulation
Regional transport
Source apportionment
Lagoon of Venice

ABSTRACT

This study combines a set of chemometric analyses with a source apportionment model for discriminating the weather conditions, local processes and remote contributions having an impact on particulate matter levels and chemical composition. The proposed approach was tested on PM_{10} data collected in a semi-rural coastal site near Venice (Italy). The PM_{10} mass, elemental composition and the water soluble inorganic ions were quantified and seven sources were identified and apportioned using the positive matrix factorization: sea spray, aged sea salt, mineral dust, mixed combustions, road traffic, secondary sulfate and secondary nitrate. The influence of weather conditions on PM_{10} composition and its sources was investigated and the importance of air temperature and relative humidity on secondary components was evaluated. Samples collected in days with similar atmospheric circulation patterns were clustered on the basis of wind speed and direction. Significant differences in PM_{10} levels and chemical composition pointed out that the production of sea salt is strongly depending on the intensity of local winds. Differently, typical primary pollutants (i.e. from combustion and road traffic) increased during slow wind regimes. External contributions were also investigated by clustering the backward trajectories of air masses. The increase of combustion and traffic-related pollutants was observed when air masses originated from Central and Northwestern Europe and secondary sulfate was observed to rise when air masses had passed over the Po Valley. Conversely, anthropogenic contributions dropped when the origin was in the Mediterranean area and Northern Europe. The chemometric approach adopted can discriminate the role local and external sources play in determining the level and composition of airborne particulate matter and points out the weather circumstances favoring the worst pollution conditions. It may be of significant help in designing local and national air pollution control strategies.

1. Introduction

All over Europe, a large number of studies identified and apportioned the sources of PM for regulatory purposes and for developing and implementing policies for the human health and environmental protection. Most of these present a detailed knowledge of the chemical composition and the application of various receptor-modeling techniques to identify and quantify the main emission sources (e.g. Viana et al., 2008). However, the identification of the main sources should be only a starting point to characterize the space distribution and variability of PM as other factors strongly contribute to the levels of PM and influence the processes at various scales: from local, to regional, to long-distance. Among those, local

* Corresponding author. Tel.: +39 041 234 8522; fax: +39 041 234 8582.
E-mail address: brown@unive.it (B. Pavoni).

1352-2310/$ – see front matter © 2012 Elsevier Ltd. All rights reserved.
http://dx.doi.org/10.1016/j.atmosenv.2012.09.025

weather conditions, atmospheric circulation patterns and transboundary or regional transports of pollutants strongly interfere with the chemistry of aerosol generation and its subsequent atmospheric evolution, through the ageing of air masses. For example, Southern European countries can be affected by the influence of African dust outbreaks (Pederzoli et al., 2010; Remoundaki et al., 2011), although other sources can also be potentially relevant under specific weather conditions. These include sea spray under high wind regimes (Lewis and Schwartz, 2004), pollutant transports from external sources (Baker, 2010) or secondary aerosol formation processes in air masses coming from polluted areas (Squizzato et al., 2012). Nevertheless, weather conditions are not adequately considered in source apportionment studies.

Recently, the authors applied a factor–cluster analysis on chemical PM_{10} data to group samples on the basis of their similar chemical composition and origin (Masiol et al., 2010, 2012). Differences in wind roses and back-trajectories between groups have been subsequently used to identify potential sources and highlight possible relationships between weather conditions and PM_{10} variations. In the present study, a novel approach was tested to assess the contributions of local and external sources of PM_{10}, based on the application of chemometric procedures to source apportionment data. A first identification of the most probable emission sources was accomplished by applying the positive matrix factorization (PMF) model. The source apportionment results were interpreted on the basis of the most relevant weather parameters (air temperature, rain, relative humidity and solar radiation). A cluster analysis (CA) on wind data was then used to identify groups of days with similar atmospheric circulation patterns. The variations in PM_{10} levels and chemistry for each identified group were then examined to extract additional information on the most probable source locations and assess the influence of wind dynamics on air quality. A second CA was carried out on the back-trajectories to merge samples with similar air mass histories. The chemical composition of each group was then analyzed to evaluate the potential impact of regional and transboundary sources.

The proposed approach, used in the framework of source apportionment studies, can discriminate the influence of meteorological conditions in the events that PM exceeds the limits, can lead to improved understanding of the aerosol generation processes and, finally, provide a more reliable basis for mitigation strategies.

2. Study area

PM_{10} data were collected in a semi-rural coastal site near Venice (Italy), where pollution limits fixed by the European Directives are frequently exceeded because of several emission sources (ARPAV, 2010; EEA, 2012): an extended urban area with ~270,000 inhabitants and the related road, maritime and airport traffic, an industrial zone including chemical and steel plants, an oil-refinery, incineration facilities, thermoelectric power plants, glass factories (Rampazzo et al., 2008a,b). Recently, it was observed that Venice is also an ideal place to study the effects of the atmospheric circulation and the long-range transports in the Po Valley as strongly influenced by local aerosol generation processes (e.g., sea spray) and regional-scale transports of primary and secondary pollutants (Masiol et al., 2010, 2012; Squizzato et al., 2012).

3. Materials and methods

3.1. Sampling, analytical procedures and QA/QC

A PM_{10} sampling campaign was carried out from May 2007 to January 2008, to be representative of all seasons, and to include different weather and atmospheric circulation patterns. About two hundred samples (24 h) were collected with a low-volume automatic sequential sampler (Skypost, TCR Tecora, Italy) on polycarbonate Nuclepore membranes (0.4 μm pore size; GE, USA). Filters were weighed in a controlled clean room (20 ± 5 °C and 50 ± 5% relative humidity) before and after sampling, by using a microbalance. Samples were then analyzed for both water-soluble inorganic ions and elemental composition. Half filter was ultrasonically extracted with ultrapure water (specific resistivity ≈ 18 MΩ cm) and filtered through prewashed Teflon membranes (pore size 0.45 μm, PALL, USA). The aqueous extracts were then analyzed by an ion chromatographic system (model DX500, Dionex, USA) to determine the concentrations of six major inorganic ions (Cl^-, NO_3^-, SO_4^{2-}, Na^+, Mg^{2+}, NH_4^+). Samples were also analyzed for 16 elements with atomic number ≥13 (Al, Si, P, S, Cl, K, Ca, Ti, V, Cr, Mn, Fe, Ni, Cu, Zn, Br) using the Particle Induced X-ray Emission technique (PIXE) at the AN2000 Van de Graaff accelerator of INFN Legnaro laboratories (Padua, Italy). The GUPIX code was used to fit the X-ray energy spectra and calculate concentrations, errors and detection limits (DLs). More details of both analytical procedures and instrumental setup are given in Masiol et al. (2010).

Filter blanks and field blanks were used to detect sample contamination and the obtained values were routinely subtracted from those of the samples. For ion chromatography, single- and multi-ionic standards (Fluka-Riedel de-Haën, Germany) were used to test the linearity and calibrate the instrumental responses. The quality and accuracy of quantitative analyses for some ions were checked by analyzing the SRM 1648 standard for air particulate (NIST, USA). The recovery of each ion was in the range 90–110%. The relative standard deviation of each ion determination was <5%. The quality and accuracy of quantitative PIXE analyses were checked with the SRM 2783 thin film standard for air particulate (NIST, USA).

3.2. Data treatment and uncertainty assessment for PMF

USEPA PMF version 3.0 based on multilinear engine 2 program (ME 2) was used in this study. This multivariate model was widely used as a standard method for source apportionment studies (Viana et al., 2008). Details of the model and ME 2 are given elsewhere (Paatero and Tapper, 1994; Paatero, 1997; USEPA, 2008). PMF needs both species concentrations at receptor site and associated uncertainties: some methods to manage the dataset and to calculate the uncertainties are summarized in Reff et al. (2007). In this study, missing data were preliminarily treated following three approaches: i) eliminating samples for which any measurement was missing, ii) replacing missing data with the arithmetic mean or iii) the median of the remaining cases. As the approaches have not returned significantly different results, the arithmetic mean was selected and the assigned uncertainty was tripled. Uncertainties for PIXE data were handled according to Polissar et al. (1998): for data above the DLs, uncertainties were determined by compounding errors from the most uncertain components (PIXE errors, air sampled volumes and contaminations found in the field blanks) with the addition of 1/3 of the DLs. Concentrations below the DLs or with PIXE errors >50% were set as DL/2, with an uncertainty of 5/6 of the corresponding element DL. Uncertainties associated to ion determinations were estimated using the equation-based method (USEPA, 2008) with an error fraction computed by compounding the variation on four different water extraction of SRM, field blank errors and sampled air volumes. Common uncertainties were found in the range of 7–20% for SO_4^{2-} and Mg^{2+}, respectively.

3.3. Local weather conditions and cluster analysis on wind data

Common weather data including wind speed (m s^{-1}) and direction (degree), air temperature (°C), relative humidity (%), solar

radiation (W m^{-2}) and precipitations (mm) were hourly measured at a station near the sampling site. Wind data were homogenized and some corrections were applied when necessary: wind speeds <0.5 m s^{-1} (anemometer DLs) were assumed as wind calm, uncertain data or hours with fast changes in wind direction were excluded from the analysis.

The hourly data of wind speed and direction from the weather station were processed by extracting their scalar components *u* and *v* relative to the North–South and West–East axes (Kaufmann and Whiteman, 1999; Darby, 2005). For the purpose of this study, the hourly values of the components were separately summed to obtain a daily data, which represents the resultant vector of the air movement. A hierarchical cluster analysis using the Ward's method and the squared Euclidean distance measure were then performed on these components.

3.4. The analysis of backward trajectories

Back-trajectories were simulated at 00:00, 06:00, 12:00 and 18:00 h UTC for each sampling day by using the model NOAA/ARL HYSPLIT version 4.9 (Rolph, 2012; Draxler and Rolph, 2012) and the NCEP/NCAR Reanalysis data processing unit. The backward trajectory timescale was set at 96 h as an acceptable compromise between the accuracy, which strongly decreases with time, and the time needed to investigate the secondary aerosol formation processes. As some studies detected limitations in accuracy of trajectories calculations (Stohl, 1998), the confidence of back-trajectories was tested by using different starting heights and hours. Days with high variability in trajectories were excluded from the computations. Air trajectories were then analyzed using the HYSPLIT clustering algorithm (Draxler et al., 2009).

4. Results and discussion

4.1. Overview of PMF results

Analytical results are summarized in Table 1. Sea-salt sulfates ($ssSO_4^{2-}$) were indirectly calculated from Na^+ concentrations using the seawater ratio (0.25) and the results were subtracted from the total sulfates to obtain the non-sea-salt sulfates ($nssSO_4^{2-}$). A preselection of variables to be processed in the PMF model was made to exclude chemically redundant species (Reff et al., 2007). Sulfate and Cl^- and not total sulfur and total chlorine were chosen because of the high correlations (Pearson's $r_{S/Sulfate} = 0.7$; $r_{Cl/Cl^-} = 0.9$) and for being better representative of secondary processes and sea-salt contribution, respectively. Due to the number of samples below the DLs and following the signal-to-noise ratio criterion (Paatero and Hopke, 2003), phosphorus and bromine were excluded from the model, whereas Mg^{2+} was included as "weak" by tripling its uncertainty. An additional 10% uncertainty was added because of possible artifacts due to the use of polycarbonate membranes. These are reported to undergo a loss of aerosol mass, if compared to quartz fiber filters (Müller et al., 2004).

The definitive PMF dataset included 193 cases and 19 variables. Several runs of PMF were performed to explore the data, minimize the object function *Q* and obtain the appropriate number of factors, on the basis of the previous knowledge of impacting sources. As the theoretically optimum value of *Q* should be roughly equal to the number of elements (3667 in this case), the most physically plausible results were obtained with a seven factor solution: the predicted PM_{10} mass concentrations well reproduce the measured ones ($r^2 = 0.7$) and the scaled residuals are normally distributed. Rotational ambiguities were detected by checking the G-space plots (Paatero et al., 2005) and running solutions for multiple values of FPEAK (between −1 and +1 steps of 0.2): results were examined and the most reasonable solution was found for FPEAK = 0. The uncertainties in the modeled solution were assessed by bootstrapping the results: 200 runs were performed (minimum $r^2 = 0.6$), all runs converged and all species had stable results.

Table 1
Basic statistics of analyzed parameters (in ng m^{-3}).

	N (%) samples > LDs	Mean	Std. Dev.	Median	25%–75% percentile
PM_{10}	193 (100%)	22,450	12,880	18,637	13,720–29,174
Al	178 (92%)	164	180	104	50–185
Si	193 (100%)	410	420	265	143–472
P	114 (59%)	22	22	16	7–27
S	193 (100%)	1430	939	1181	751–1936
Cl	188 (97%)	696	1167	132	34–808
K	187 (97%)	301	404	192	119–302
Ca	193 (100%)	609	503	458	300–702
Ti	192 (99%)	16	14	11	8–19
V	156 (81%)	6	7	3	1–8
Cr	178 (92%)	3	3	2	1–3
Mn	177 (92%)	8	9	6	4–10
Fe	193 (100%)	253	256	177	116–294
Ni	153 (79%)	4	6	3	1–5
Cu	189 (98%)	9	12	5	4–9
Zn	177 (92%)	33	37	24	11–39
Br	79 (41%)	7	7	5	3–9
Cl^-	181 (94%)	680	1162	160	31–731
NO_3^-	189 (98%)	2255	3765	1096	446–2179
SO_4^{2-}	190 (98%)	3749	2458	3432	1758–5271
Na^+	189 (98%)	1050	1164	684	382–1181
Mg^{2+}	186 (96%)	207	204	140	91–236
NH_4^+	184 (95%)	1322	1558	827	248–1872

The interpretation of extracted sources was based on the presence of some well-known markers and the findings of other studies in the area. Fig. 1 shows the resolved factor chemical profiles (percent mass of each chemical species) and the total mass variation in time, whereas the factor profiles (concentration of species and percent of total species) in numeric form are reported as supplementary material. Results are in general agreement with previous studies (Rampazzo et al., 2008a,b; Masiol et al., 2010), but some additional sources have been identified. The first source clearly reflects the sea-spray composition, having high shares of chlorine (90% of Cl^- mass), sodium (44%) and magnesium (35%), and a considerable content of calcium (7%). The second source is mainly composed of potassium (76%), a typical tracer for biomass burning (Puxbaum et al., 2007; Saarnio et al., 2010), copper (22%), calcium (18%) and titanium (18%) and was attributed to mixed combustion processes. The third source contains high percentages of Zn (93%), Mn (62%), Cr (59%), Cu (55%), Fe (44%), Ni (21%) and Ca (17%) suggesting the road traffic as the most probable origin (Sternbeck et al., 2002; Amato et al., 2011).

The fourth source is dominated by SO_4^{2-} (58%), Na^+ (50%) and Mg^{2+} (45%) with moderate percentages of Ni (17%) and V (16%). As observed for the first source, sodium and magnesium are typical tracers for sea spray, but chloride is missing and sulfate overabundant. It has been demonstrated that sometimes sea salt aerosols may show a large chloride deficiency compared to the original seawater composition (Rossi, 2003; Seinfeld and Pandis, 2006). This Cl^- deficit (named chloride depletion) is generally attributed to a series of chemical reactions involving alkali halides and strong inorganic acids, such as HNO_3 and H_2SO_4 in both gaseous and aqueous phases (ten Brink, 1998) and occurs predominantly in the coarse particle mode (Zhao and Gao, 2008). In this case, an excess of atmospheric sulfuric acid has probably

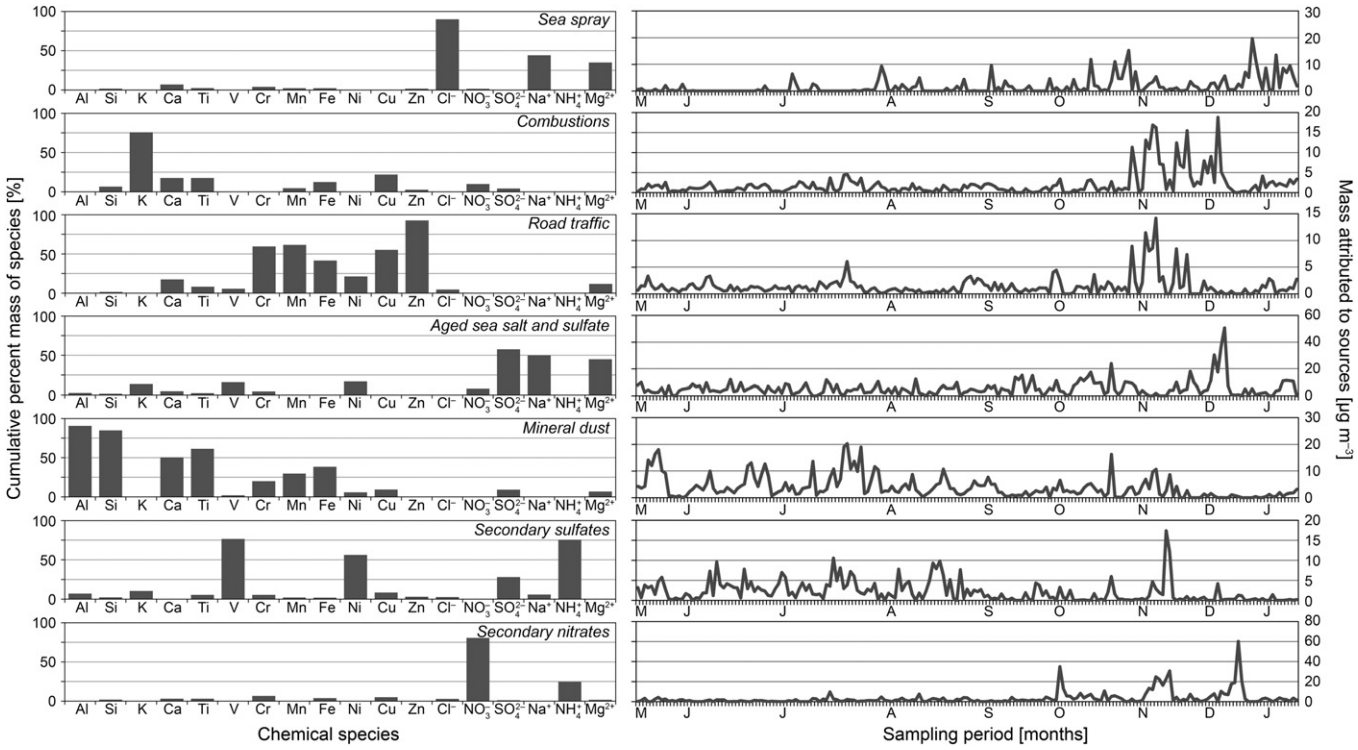

Fig. 1. Cumulative percent mass of species (left) and resulting time series (right) for the seven sources identified by the PMF. The time scales show only the days really sampled and the resulting scale is not linear.

reacted with fresh sea salt particles resulting in the formation of sulfate salts:

$$2NaCl_{(s)}+H_2SO_{4(g)} \leftrightarrow Na_2SO_{4(s)}+2HCl_{(g)}$$

$$NaCl_{(s)}+H_2SO_{4(g)} \leftrightarrow NaHSO_{4(s)}+HCl_{(g)}$$

It is therefore reasonable to relate this source to the ageing of sea-salt aerosols i.e. to heterogeneous reactions with atmospheric S(VI), from the oxidation of S(IV) species. The concurrent presence of moderate V and Ni shares in this source leads to the assumption that sulfate has an anthropogenic origin from fuel combustion and transformation processes.

The fifth source carries high percentages of Al (91%), Si (85%), Ti (61%), Ca (50%), Fe (38%) and Mn (30%). These are the major constituents of soil and point out the fingerprint of mineral dust. This may have also originated from various processes which were active in the sampling period: (i) engineering works for the construction of high-tide preventing dams at the Venice Lagoon entrance were in progress; (ii) the glass factories in the Island of Murano typically emit crustal raw materials (Rampazzo et al., 2008a); (iii) Saharan dust may have occasionally reached the sampling station (Masiol et al., 2010).

The last two sources are clearly related to the formation of the secondary inorganic aerosol (SIA) in the atmosphere through (photo-) chemical reactions of some gaseous precursors. The sixth factor is characterized by high shares of ammonium (76%), sulfate (28%) and also V (77%) and Ni (56%) reflecting the formation of ammonium sulfate ($(NH_4)_2SO_4$) and ammonium hydrogen sulfate (NH_4HSO_4). These salts are generated by the ternary nucleation of H_2SO_4, NH_3, and H_2O in the atmosphere and were detected all over Europe (Viana et al., 2008). The major precursor of sulfuric acid in the continental troposphere is sulfur dioxide (SO_2), which is oxidized in the daytime by hydroxyl radicals (Seinfeld and Pandis, 2006). As evidenced by the yearly emission inventory published for the Venice area in 2005 by Italian authorities (ISPRA, 2012), this gas is largely emitted by combustions from energy and transformation industries (19.6 Gg), manufacturing industries (2 Gg) and production processes (1.6 Gg), which also emit vanadium and nickel (Bosco et al., 2005; Alastuey et al., 2007). The gaseous ammonia originates mainly from agriculture (4.3 Gg) and secondarily from road transport (0.2 Gg).

The seventh source is made up of nitrate (81%) and ammonium (24%), i.e. the components of secondary ammonium nitrate (NH_4NO_3) formed through both homogenous and heterogeneous reactions. In the daytime, a large amount of HNO_3 is generated by the reaction between NO_2 and •OH, and directly reacts with gaseous NH_3. In contrast, in the nighttime the generation of the nitrogen pentoxide (N_2O_5) formed by the reaction between NO_3 and NO_2 radicals and its subsequent hydrolysis become the principal way of particulate nitrate formation (Seinfeld and Pandis, 2006). In short, the main gaseous precursors of atmospheric nitric acid are the nitrogen oxides (NO_x). These in the Venice area are mainly emitted from combustions in energy and transformation industries (12.2 Gg) and road transport (8.1 Gg). An additional amount of 9 Gg is attributed to non-industrial combustion plants, combustion in manufacturing and other mobile sources and machinery (ISPRA, 2012).

On an annual basis, the largest source contributing to PM_{10} mass was aged sea salt and sulfate, accounting for 5.5 μg m^{-3} (25%), followed by mineral dust (3.9 μg m^{-3}, 19%), secondary nitrate (3.3 μg m^{-3}, 17%), secondary sulfate (2.1 μg m^{-3}, 10%), mixed combustions (2.1 μg m^{-3}, 10%), sea spray (1.7 μg m^{-3}, 8%) and road traffic (1.4 μg m^{-3}, 7%). The annual source contributions and the seasonal trends were also examined to highlight the changes in source apportions due to different weather conditions. Fig. 2 presents the cumulative percentage evidencing that sea spray reaches the highest relative levels (~20% of total PM_{10} mass)

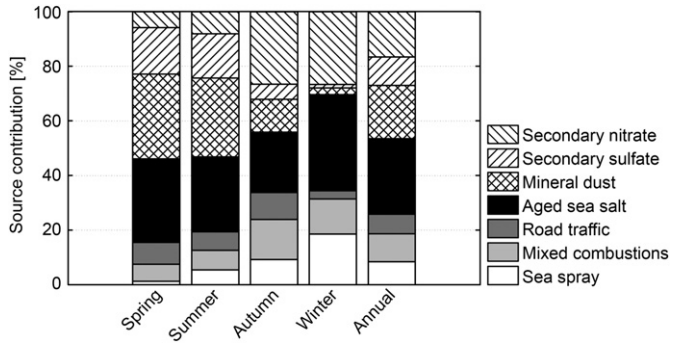

Fig. 2. Seasonal and annual source contributions (cumulative percentage) from PMF.

during winter, mineral dust has a larger relative apportion in spring (31%) and summer (29%), and the aged sea salt is almost constant during the whole year. As expected, mixed combustions increase their relative importance in autumn and winter, due to domestic heating and agricultural biomass burning in the surrounding area. Fig. 2 also emphasizes the clear seasonality of secondary inorganic aerosols, with major contributions of ammonium sulfate during the warmest periods and a prevalence of ammonium nitrate during the cold season.

4.2. Relationship of PM with weather conditions

A search for relationships between PM_{10} levels, source contributions estimated by PMF and daily mean values of wind speed, air temperature, relative humidity, solar radiation and daily precipitation was performed by means of Pearson correlations (Table 2). On an annual basis, air temperature and solar radiance show moderate negative correlations (significant at $p < 0.0001$) with sea spray, mixed combustions and secondary nitrate, and positive with crustal dust and secondary sulfate. The inverse relationships of sea spray with temperature and solar radiation can be related to the increased wind speed and the less intense chlorine depleting photochemical processes of the cold season. The negative correlation between temperature and mixed combustions can also be attributed to the increased domestic heating emissions in the wintertime. On the contrary, the positive correlations between air temperature and solar radiation with mineral dust could be related to the enhanced wind erosion occurring in the warmest periods when the upper soil dries up and is pulverized.

Table 2
Pearson correlation coefficients between weather parameters, modeled source contributions and measured PM_{10}. Bold face correlations are significant at $p < 0.0001$.

	Wind speed	Air temperature	Solar radiation	Relative humidity
Wind speed ($m\ s^{-1}$)	1			
Air temperature (°C)	−0.01	1		
Solar radiation ($W\ m^{-2}$)	−0.01	**0.84**	1	
Relative humidity (%)	**−0.37**	**−0.29**	**−0.48**	1
Sea spray ($\mu g\ m^{-3}$)	**0.39**	**−0.43**	**−0.42**	0.06
Mixed combustions ($\mu g\ m^{-3}$)	−0.23	**−0.35**	**−0.34**	0.06
Road traffic ($\mu g\ m^{-3}$)	**−0.29**	−0.09	−0.10	0.00
Aged sea salt and sulfate ($\mu g\ m^{-3}$)	−0.08	−0.16	−0.15	0.16
Mineral dust ($\mu g\ m^{-3}$)	−0.08	**0.50**	**0.38**	−0.21
Secondary sulfate ($\mu g\ m^{-3}$)	−0.16	**0.38**	**0.37**	0.06
Secondary nitrate ($\mu g\ m^{-3}$)	−0.24	**−0.35**	**−0.35**	**0.31**
Measured PM_{10} ($\mu g\ m^{-3}$)	−0.24	−0.17	−0.26	**0.31**

Secondary sulfate and nitrate have opposite behaviors with air temperature and solar radiation. The time variations plotted in Fig. 1 and the seasonal source contributions in Fig. 2 show that secondary sulfate formation is dominant during the warm period (June–August), whereas secondary nitrate reaches its highest concentrations during the coldest months (November–January), as expected from the chemistry of SIA formation processes: Schaap et al. (2004) evidenced that ammonium nitrate inversely follows the air temperature, with higher levels during cold periods. Its generation is favored by lower air temperatures and higher levels of precursor NO_x from domestic heating. Moreover, being NH_4NO_3 unstable under normal atmospheric conditions, the increased air temperature may favor the partitioning into the gaseous phase and therefore the mass reduction of aerosol nitrate (Dawson et al., 2007). In contrast, higher temperatures by enhancing the oxidant concentrations and the gas-phase reaction rates, produce higher atmospheric sulfate concentrations (Pye et al., 2009 and reference therein).

Relative humidity has a slight positive correlation with secondary nitrate and PM_{10} mass. This result is explained by the ammonium nitrate reactivity, which is favored not only by low temperatures but also by high relative humidity conditions (Stelson and Seinfeld, 1982). The moderate positive correlation between the relative humidity and PM_{10} mass can be mainly attributed to the concurrent increase of water content and mass in the particles. Since rain data are affected by many zero values, they were treated separately. Results show that on an annual basis PM_{10} is moderately influenced by precipitation rates, with a slight decrease on occasion of strong precipitation events.

4.3. Cluster analysis on wind data

The *q*-mode CA on the *u* and *v* components of wind data was performed and the resulting dendrogram is reported as supplementary material. Four clusters identifying four groups of samples were detected with a normalized $(D_{link}/D_{max})^*100$ cut-off of 20, which represents the similarity value. Average wind speeds ($\bar{u}$) and predominant directions of each identified group were then compared with the full period (Fig. 3). In the same way, the corresponding differences in PMF results among extracted groups are also reported as boxplots in Fig. 3 to highlight the potential influence of the local atmospheric circulation on the PM_{10} levels and composition.

Group 1 ($N = 16$) shows prevailing wind from the first quadrant, with very high average speeds (3 $m\ s^{-1}$) and 1% calm hours. Fast winds from NE (called "bora") form peculiar cold and gusty downslope windstorm blowing over the Adriatic and bringing air masses from Northern Europe. From the boxplots it is evident that these conditions may cause a strong increase of sea-spray (percent difference compared to the mean of all groups $(\bar{x}_i - \bar{x}_{1\ldots4}/\bar{x}_{1\ldots4}) + 260\%$) and the drop of anthropogenic pollutants (combustion, road traffic, −52% and −57%, respectively).

Group 2 ($N = 32$) also presents winds blowing from first quadrant, but with moderate speeds ($\bar{u} = 1.6\ m\ s^{-1}$). This pattern is frequent during the cold season (2/3 of samples in this group were collected between October and January) when sea/land breezes are absent. For this group, the modeled sea salt contributions are definitely lower than for the first one as the marine aerosol generation is strongly wind speed-dependant (Lewis and Schwartz, 2004). However, this group has also a strong decrease of secondary sulfate (−69%) and a moderate increase of aged sea salt (+12%) with respect to the full period, suggesting that these conditions may favor chlorine losses.

Group 3 ($N = 73$) shows two predominant wind directions, quadrant I and II, with no significant differences in wind calm hours and the average speed compared to the full period. The direction

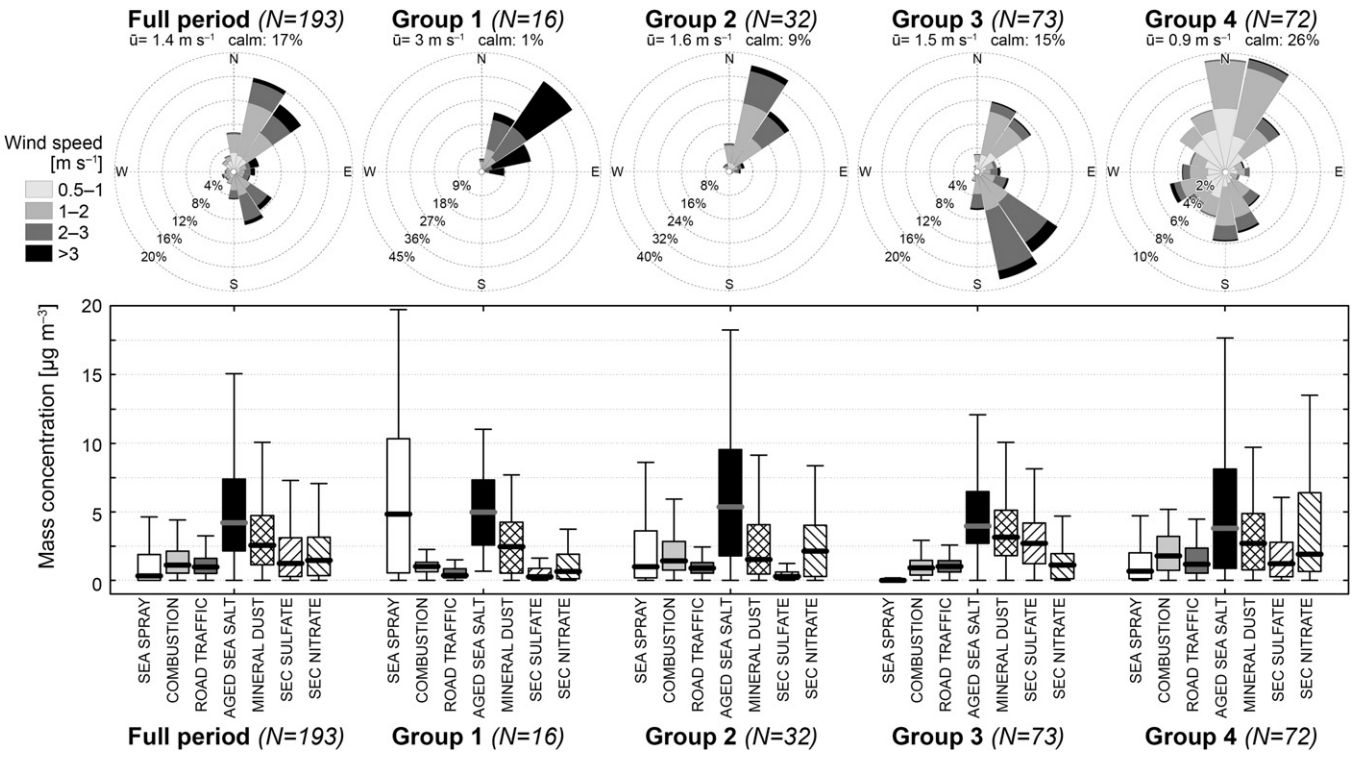

Fig. 3. Wind roses (upper) and boxplots for modeled source contributions (bottom) for the groups extracted by clustering the wind data.

from quadrant II occurs mainly during the warm season and is typically due to the sea-breeze circulation. It can also be due to a peculiar wind pattern called "scirocco", which brings warm air masses from southern Adriatic and Mediterranean regions. As evidenced in previous studies (Masiol et al., 2010), these conditions lead to a significant rise of modeled secondary sulfate contributions (+48%). In addition, a moderate increase of mineral dust levels (+13%) was observed along with the drop of other sources: sea spray (−68%), mixed combustions (−40%), secondary nitrate (−50%). This scenario was attributed to the peculiar air mass circulation over the Adriatic sea: the nocturnal land breezes from NE force pollutants emitted in continental areas to be driven toward the open sea, where gaseous pollutants are converted via gas-to-particle reactions and cause ammonium sulfate generation. The following diurnal sea breezes from the SE force these polluted air masses to go back from sea to land.

The last group ($N = 72$) shows air mass stagnation regimes having low wind speeds (<1 m s^{-1}), high percentage of wind calm (26%) and no prevailing directions. However an increase of winds blowing from the main local emission sources (i.e. from the third and fourth quadrants) was monitored. The study area is in some periods affected by prolonged atmospheric neutrality and stability during several consecutive days (Rampazzo et al., 2008b), that creates an air stratification and forces air masses into prevailingly horizontal displacements with low wind speeds. These conditions decrease the mechanical turbulent dispersion and tend to trap pollutants emitted locally. This fact is clearly reflected by the PMF results, showing significant increases of pollution-related sources: combustions (+42%), road traffic (+31%), secondary nitrate (+64%) and the average PM_{10} levels (26 µg m^{-3}) as well.

4.4. Backward trajectories of air masses

In this study, five trajectories were simulated per day and to each of them the daily PM_{10} and the modeled source contributions were attributed. A total of 772 daily trajectories were clustered and the optimal number of cluster was chosen by analyzing the change in the total spatial variance: the average trajectories of the seven clusters retained are shown in Fig. 4. All clusters have a significant number of observations (>5%, i.e. about 10 days) except those from the Arctic regions; these were excluded from the following statistics. The boxplots in the same Fig. 4 show the differences of modeled source contributions of the sample groups compared with the full period. Cluster 1 accounting for 19% of the observations, includes trajectories from Northwestern Europe and has no evident difference with the full period: a scarce influence of external transports from this part of Europe is apparent. Trajectories of cluster 2 (25%) originating from the Central Europe reveal a possible transport of pollutants from this area in days characterized by the largest average contributions of both mixed combustions and road traffic (on average +28% and +29%, respectively) and also of aged sea salt and mineral dust (+17%). Cluster 3 is the most frequent (34%) and groups air masses passing over the Po Valley. The average modeled contributions are the highest for mineral dust (+44%) and secondary sulfate (+57%) evidencing a potential influence of regional-scale transports. The rise of mineral dust can be linked to land use of intensive agriculture in the rural areas of the plain. Differently, the increased secondary sulfate can be related to the emission of gaseous precursors from fossil fuels in the anthropized areas of the Po Valley. Cluster 4 (8%) shows a Mediterranean provenance, has low mass contributions of mineral dust (−29%), secondary sulfate (−33%) and a high sea salt apportion (+109%). Also a moderate contribution of marine aerosol from this region is likely. Cluster 5 (6%) includes trajectories coming from the Atlantic region and passing over the Western Europe. It presents increased concentrations of secondary nitrate (+184%) as already reported in Squizzato et al. (2012). The last significant cluster accounts for 6% of total sampling days and includes trajectories from the Northern Europe. Modeled source contributions show that on an average this

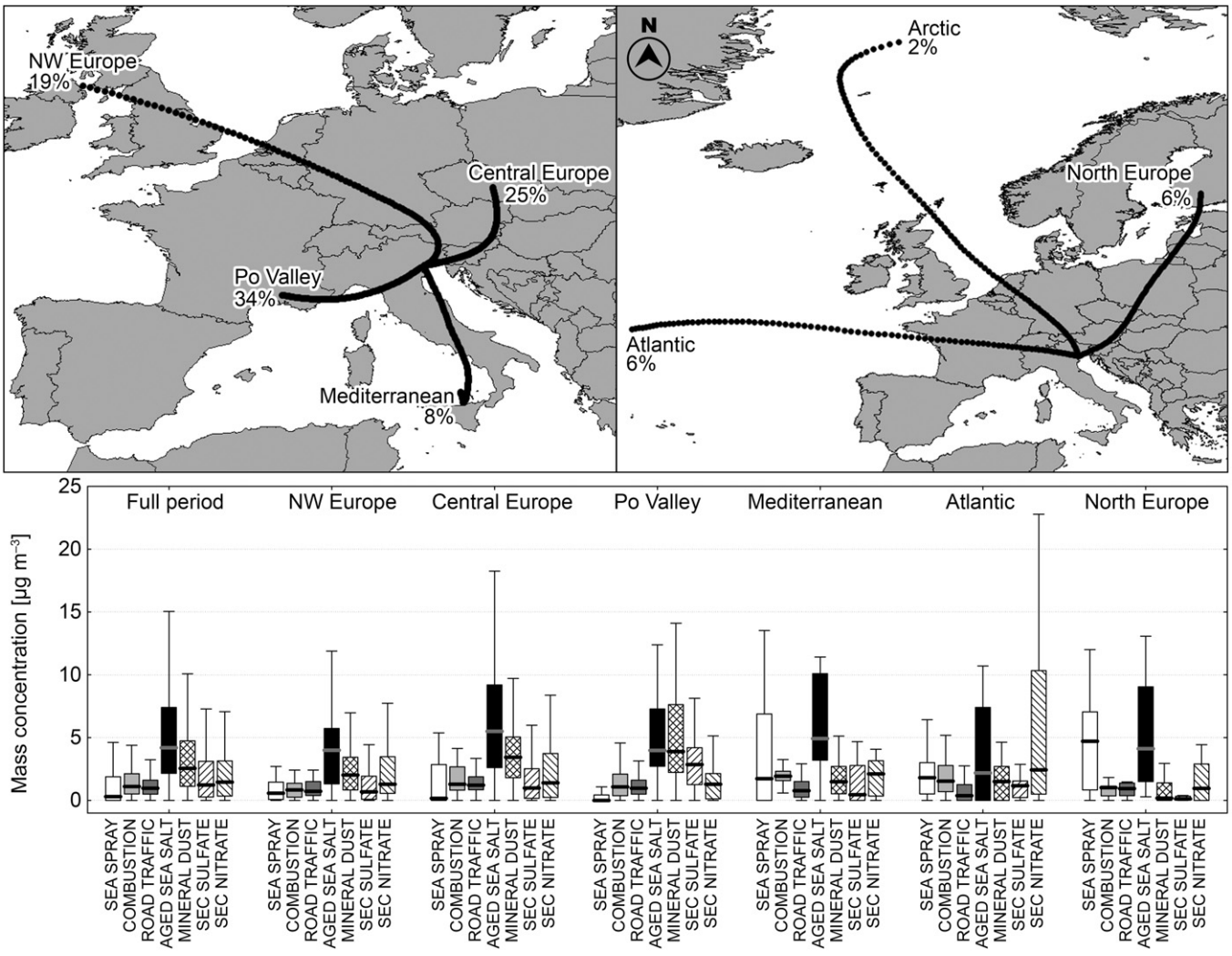

Fig. 4. Results of the cluster analysis on the air mass backward trajectories (upper) and their relative boxplots for the modeled source contributions (bottom).

group presents a strong increase of fresh sea salt (+231%) and an evident drop of mineral dust (−81%), secondary sulfate (−91%) and secondary nitrate (−44%). However, the increase of marine aerosol can be attributed to local generation processes on occasion of "bora" episodes as supported by the fact that days in this cluster also exhibit high wind speed.

These results witness a convincing influences of long-range transports on the PM_{10} levels and composition in the study area. Generally, pollution-related components slightly increase when air masses come from Central Europe, whereas the secondary sulfate component significantly increase when air masses pass over the Po Valley. On the contrary, a decrease of pollutants is evident when air masses originate from Northern Europe.

5. Conclusions

This study combines a source apportionment procedure with some chemometric tools to identify and quantify the local and external contributions to PM_{10} levels and chemistry. This approach was tested on data collected in four seasons (2007–2008) in a semi-rural coastal site located in the Eastern part of the Po Valley. From a PMF receptor model seven factors were characterized and apportioned. Annually, aged sea salt and sulfate contributed to most of PM_{10} mass followed by mineral dust, secondary nitrate, secondary sulfate, mixed combustions, sea spray and road traffic. The influence of weather parameters on PM_{10} and sources was studied and the importance of air temperature and relative humidity on secondary components was evident.

The role of both local air circulation and long-range transports were then studied by clustering wind data and backward trajectories, respectively, and by analyzing the variations in source contributions. The cluster analysis on wind data extracted four groups from the entire set of observations: fast winds blowing from NE, moderate winds from NE, sea/land breeze circulation pattern and air mass stagnation. Results show that sea spray levels are strongly influenced by local weather conditions, having the highest levels during windy days, whereas combustions and road traffic increase during stagnation conditions. In addition, the differences in the modeled source contributions were assessed in combination with the clustering of air mass backward trajectories. Results pointed out a potential influence of long-range transports on the PM_{10} levels and composition in the study area. In particular, pollution-related components slightly increased when air masses were coming from Central Europe, whereas the secondary sulfate component was observed to increase significantly when air masses had spent most of their time over the Po Valley. Differently, air mass from Northern Europe generally were less pollutant loaded.

The combination of the proposed procedures has extracted interpretable information on PM origins and assessed the influence of weather conditions on the PM_{10} levels and composition. This study has also allowed an evaluation of the main local, regional and transboundary processes that may have an effect on PM_{10} composition, by revealing the changes in the source contributions during different atmospheric circulation patterns and external transport episodes.

The proposed approach may be easily adapted to other environmental contexts to better interpret the source apportionment results and be a handy tool in planning local and national air pollution control measures.

Acknowledgment

This study is part of a PhD thesis financed by the Italian Ministry of Education, University and Research (MIUR). The authors are grateful to Laboratori Nazionali di Legnaro of INFN (http://www.lnl.infn.it) for PIXE, Dr. Elena Ghedini (Università Ca' Foscari Venezia) for her analytical support, ARPAV-Centro Meteorologico di Teolo (http://www.arpa.veneto.it/teolo/html/finale_it/informazioni.html) for weather data and Comando Zona Fari e Segnalamenti Marittimi di Venezia for logistics. The authors gratefully acknowledge the NOAA Air Resources Laboratory (ARL) for the provision of the HYSPLIT transport and dispersion model and/or READY website (http://www.arl.noaa.gov/ready.php) used in this publication.

Appendix A. Supplementary data

Supplementary data related to this article can be found at http://dx.doi.org/10.1016/j.atmosenv.2012.09.025.

References

Alastuey, A., Moreno, N., Querol, X., Viana, M., Artíñano, B., Luaces, J.A., Basora, J., Guerra, A., 2007. Contribution of harbour activities to levels of particulate matter in a harbour area: Hada Project-Tarragona Spain. Atmospheric Environment 41, 6366–6378.

Amato, F., Pandolfi, M., Moreno, T., Furger, M., Pey, J., Alastuey, A., Bukowiecki, N., Prevot, A.S.H., Baltensperger, U., Querol, X., 2011. Sources and variability of inhalable road dust particles in three European cities. Atmospheric Environment 45, 6777–6787.

ARPAV (Environmental Protection Agency of Veneto Region), 2010. The Quality of the Air in the Municipality of Venice. Annual Report 2009, p. 113 (in Italian).

Baker, J., 2010. A cluster analysis of long range air transport pathways and associated pollutant concentrations within the UK. Atmospheric Environment 44, 563–571.

Bosco, M.L., Varrica, D., Dongarrà, G., 2005. Case study: inorganic pollutants associated with particulate matter from an area near a petrochemical plant. Environmental Research 99, 18–30.

Darby, L., 2005. Cluster analysis of surface winds in Houston, Texas, and the impact of wind patterns on ozone. Journal of Applied Meteorology 44, 1788–1806.

Dawson, J.P., Adams, P.J., Pandis, S.N., 2007. Sensitivity of $PM_{2.5}$ to climate in the eastern U.S.: a modeling case study. Atmospheric Chemistry and Physics 7, 4295–4309.

Draxler, R.R., Rolph, G.D., 2012. HYSPLIT (HYbrid Single-particle Lagrangian Integrated Trajectory) Model access via NOAA ARL READY Website. NOAA Air Resources Laboratory, Silver Spring, MD. http://ready.arl.noaa.gov/HYSPLIT.php.

Draxler, R., Stunder, B., Rolph, G., Stein, A., Taylor, A., 2009. HYSPLIT4 User's Guide. Revision January 2009. NOAA Air Resources Laboratory. http://www.arl.noaa.gov/documents/reports/hysplit_user_guide.pdf.

EEA, European Environment Agency, 2012. AirBase—The European Air Quality Database. Available from: http://www.eea.europa.eu/themes/air/airbase (last accessed January, 2012).

ISPRA (Italian Institute for Environmental Protection and Research), 2012. Disaggregated Emission Inventory 2005. Available: http://www.sinanet.isprambiente.it/it/inventaria/disaggregazione_prov2005/ (last accessed January 2012).

Kaufmann, P., Whiteman, C.D., 1999. Cluster-analysis classification of wintertime wind patterns in the Grand Canyon region. Journal of Applied Meteorology 38, 1131–1147.

Lewis, E.R., Schwartz, S.E., 2004. Sea Salt Aerosol Production – Mechanisms, Methods, Measurements, and Models. In: Geophysical Monograph Series, vol. 152. American Geophysical Union, Washington, 413 pp.

Masiol, M., Rampazzo, G., Ceccato, D., Squizzato, S., Pavoni, B., 2010. Characterization of PM_{10} sources in a coastal area near Venice (Italy): an application of factor–cluster analysis. Chemosphere 80, 771–778.

Masiol, M., Squizzato, S., Ceccato, D., Rampazzo, G., Pavoni, B., 2012. A chemometric approach to determine local and regional sources of PM_{10} and its geochemical composition in a coastal area. Atmospheric Environment. http://dx.doi.org/10.1016/j.atmosenv.2012.02.089.

Müller, K., Spindler, G., Maenhaut, W., Hitzenberger, R., Wieprecht, W., Baltensperger, U., ten Brink, H., 2004. INTERCOMP2000, a campaign to assess the comparability of methods in use in Europe for measuring aerosol composition. Atmospheric Environment 38, 6459–6466.

Paatero, P., 1997. Least squares formulation of robust non-negative factor analysis. Chemometrics and Intelligent Laboratory Systems 37, 23–35.

Paatero, P., Tapper, U., 1994. Positive matrix factorization: a non-negative factor model with optimal utilization of error estimates of data values. Environmetrics 5, 111–126.

Paatero, P., Hopke, P.K., 2003. Discarding or downweighting high-noise variables in factor analytic models. Analytica Chimica Acta 490, 277–289.

Paatero, P., Hopke, P.K., Begum, B.A., Biswas, S.W., 2005. A graphical diagnostic method for assessing the rotation in factor analytical models of atmospheric pollution. Atmospheric Environment 39, 193–201.

Pederzoli, A., Mircea, M., Finardi, S., di Sarra, A., Zanini, G., 2010. Quantification of Saharan dust contribution to PM_{10} concentrations over Italy during 2003–2005. Atmospheric Environment 44, 4181–4190.

Polissar, A.V., Hopke, P.K., Paatero, P., Malm, W.C., Sisler, J.F., 1998. Atmospheric aerosol over Alaska 2. Elemental composition and sources. Journal of Geophysical Research 103 (D15), 19045–19057. http://dx.doi.org/10.1029/98JD01212.

Puxbaum, H., Caseiro, A., Sánchez-Ochoa, A., Kasper-Giebl, A., Claeys, M., Gelencser, A., Legrand, M., Preunkert, S., Pio, C., 2007. Levoglucosan levels at background sites in Europe for assessing the impact of biomass combustion on the European aerosol background. Journal of Geophysical Research 112, D23S05. http://dx.doi.org/10.1029/2006JD008114.

Pye, H.O.T., Liao, H., Wu, S., Mickley, L.J., Jacob, D.J., Henze, D.K., Seinfeld, J.H., 2009. Effect of changes in climate and emissions on future sulfate–nitrate–ammonium aerosol levels in the United States. Journal of Geophysical Research 114, D01205. http://dx.doi.org/10.1029/2008JD010701.

Rampazzo, G., Masiol, M., Visin, F., Rampado, E., Pavoni, B., 2008a. Geochemical characterization of PM_{10} emitted by glass factories in Murano, Venice (Italy). Chemosphere 71, 2068–2075.

Rampazzo, G., Masiol, M., Visin, F., Pavoni, B., 2008b. Gaseous and PM_{10}-bound pollutants monitored in three environmental conditions in the Venice area (Italy). Water, Air & Soil Pollution 195, 161–176.

Reff, A., Eberly, S.I., Bhave, P.V., 2007. Receptor modeling of ambient particulate matter data using Positive Matrix Factorization: review of existing methods. Journal of the Air & Waste Management Association 57, 146–154.

Remoundaki, E., Bourliva, A., Kokkalis, P., Mamouri, R.E., Papayannis, A., Grigoratos, T., Samara, C., Tsezos, M., 2011. PM_{10} composition during an intense Saharan dust transport event over Athens (Greece). Science of The Total Environment 409, 4361–4372.

Rolph, G.D., 2012. Real-time Environmental Applications and Display sYstem (READY). Website. http://ready.arl.noaa.gov. NOAA Air Resources Laboratory, Silver Spring, MD.

Rossi, M.J., 2003. Heterogeneous reactions on salts. Chemical Reviews 103, 4823–4882.

Saarnio, K., Aurela, M., Timonen, H., Saarikoski, S., Teinila, K., Makela, T., Sofiev, M., Koskinen, J., Aalto, P.P., Kulmala, M., Kukkonen, J., Hillamo, R., 2010. Chemical composition of fine particles in fresh smoke plumes from boreal wild-land fires in Europe. Science of the Total Environment 408, 2527–2542.

Schaap, M., van Loon, M., ten Brink, H.M., Dentener, F.J., Builtjes, P.J.H., 2004. Secondary inorganic aerosol simulations for Europe with special attention to nitrate. Atmospheric Chemistry and Physics 4, 857–874.

Seinfeld, J.H., Pandis, S.N., 2006. Atmospheric Chemistry and Physics, second ed.. In: From Air Pollution to Climate Change John Wiley & Sons, NewYork.

Squizzato, S., Masiol, M., Innocente, E., Pecorari, E., Rampazzo, G., Pavoni, B., 2012. A procedure to assess local and long-range transport contributions to $PM_{2.5}$ and secondary inorganic aerosol. Journal of Aerosol Science 46, 64–76.

Stelson, A.W., Seinfeld, J.H., 1982. Relative humidity and temperature dependence of ammonium nitrate dissociation constant. Atmospheric Environment 16, 983–992.

Sternbeck, J., Sjodin, A., Andreason, K., 2002. Metal emissions from road traffic and the influence of resuspension—results from two tunnel studies. Atmospheric Environment 36, 4735–4744.

Stohl, A., 1998. Computation, accuracy and applications of trajectories – a review and bibliography. Atmospheric Environment 32, 947–966.

ten Brink, H.M., 1998. Reactive uptake of HNO_3 and H_2SO_4 in sea-salt (NaCl) particles. Journal of Aerosol Science 29, 57–64.

USEPA (United States Environmental Protection Agency), 2008. EPA Positive Matrix Factorization (PMF) 3.0. In: Fundamentals & User Guide. USEPA Office of Research and Development, Washington DC, USA, 81 pp.

Viana, M., Kuhlbusch, T.A.J., Querol, X., Alastuey, A., Harrison, R.M., Hopke, P.K., Winiwarter, W., Vallius, M., Szidat, S., Prévôt, A.S.H., Hueglin, C., Bloemen, H., Wåhlin, P., Vecchi, R., Miranda, A.I., Kasper-Giebl, A., Maenhaut, W., Hitzenberger, R., 2008. Source apportionment of particulate matter in Europe: a review of methods and results. Journal of Aerosol Science 39 (10), 827–849.

Zhao, Y., Gao, Y., 2008. Acidic species and chloride depletion in coarse aerosol particles in the US east coast. Science of the Total Environment 407, 541–547.